JOURNAL OF AIRCRAFT
Vol. 31, No. 6, November–December 1994

Sidewash on the Vertical Tail in Subsonic and Supersonic Flows

Chyn-shan Chiu*
China Junior College of Technology, Taipei, Taiwan, Republic of China
and
I. J. Lin†
Chung Shan Institute of Science and Technology, Taichung 40722, Taiwan, Republic of China

A generalized vortex-lattice method is used for the investigation of sidewash on the single and twin vertical tails due to rolling wing in subsonic and supersonic flows. The current results of sidewash on the single vertical tail in incompressible inviscid flow are almost the same as Michael's calculations. The sidewash on the single vertical tail through high angle of attack is presented. The difference of sidewash on the single and twin vertical tail that is induced by the rolling wing in subsonic and supersonic flows is also studied.

Nomenclature

AR = aspect ratio, b^2/S
B = $-\beta^2$, definitely positive
C = constant; $c = 1$ as $M_\infty < 1$, $c = 0$ as $M_\infty > 1$
c = mean aerodynamic chord of wing
$\bar{c}$ = local wing chord
D = influence coefficient matrix, depends on wing geometry
h = distance, measured in $X'Z'$ plane, perpendicular to longitudinal stability axis, positive above longitudinal axis
h_t = tail height measured in XZ plane, positive above vortex sheet
j = jth vortex element
K = constant; $K = 1$ for subsonic flows, $K = 2$ for supersonic flows
l_t = tail arm, measured from $(\bar{c}/4)$ of wing to c.p. of vertical tail
M = Mach number
N = total number of wing element
p = rolling velocity
$(pb/2V)$ = rolling velocity parameter
R_β = real part of $\{(x - x_1)^2 + \beta^2[(y - y_1)^2 + z_1^2]\}^{1/2}$
$\boldsymbol{R}$ = position vector of point (x, y, z)
$\boldsymbol{R}_1$ = position vector of point (x_1, y_1, z_1)
S_j = influence coefficient, depends on wing geometry and location of point $Q(x', y', z')$
s = half-span of the jth wing element
s' = distance between the symmetric axis of jth wing element and the longitudinal symmetric plane
t = $\tan \Lambda$
u, v, w = induced velocity components in x, y, and z direction, respectively
$\boldsymbol{V}$ = perturbation velocity vector and freestream velocity
x, y, z = local Cartesian coordinate of the wing element
$x'y'z'$ = Cartesian coordinate of the airplane
y_t = lateral distance of tail
α = angle of attack
β = $\sqrt{1 - M^2}$
Γ = circulation distribution of the wing
Γ_j = circulation strength of jth wing element
$\boldsymbol{\gamma}$ = vortex density vector of filament
ε = downwash angle
Λ = angle between the y axis and the vector of the vortex element γ
$\Lambda_{c/4}$ = sweepback angle of quarterchord line of wing
λ = taper ratio of wing
λ_{LE} = sweepback angle of leading edge of wing
σ = sidewash angle

Introduction

LAN developed a program for calculating the lateral-directional dynamic derivatives of nonplanar wings by the quasi-vortex-lattice method.[1] Later he extended it to evaluate the dynamic derivatives through high angle of attack.[2] Lan's methods are limited to subsonic flow, body effects are not included. Whether the wind-tunnel data is available or not, the DATCOM method[3] is good enough for static and dynamic derivatives estimation in the airplane design stage. But the semiempirical method of DATCOM is only suitable for stability derivatives estimation at low angle of attack. For rolling dynamic derivatives evaluation, Roskam suggested a simple method[4] to calculate the vertical tail contribution, but he did not discuss the important interference effects by the wing.

Previous experience showed that a combination of "strip theory" and "component build-up method" was a good method for aircraft dynamic derivatives estimation by using the static aerodynamic data from forced model tests in a wind tunnel. Wykes et al.[5] calculated the dynamic derivatives by the methods just mentioned for the F-100D fighter in spin analysis.[5] They considered that the sidewash effect on the vertical tail due to rolling wing by Michael's[6] method was derived from the single vertical tail in incompressible inviscid flows.

Considering that modern advanced fighters always use twin vertical tails and perform high-speed maneuvers, the authors attempt to expand the previous study to calculate the sidewash on the vertical tails,[7] both in the subsonic and supersonic flight regimes. In addition, some comparisons of current calculations with Michael's results are also carried out in this article.

Analytical Method

Circulation Distribution on the Wing in Subsonic and Supersonic Flows

Weissinger[8] developed the simplest vortex-lattice method. His method, which can be applied to wings of any planform

Received Aug. 15, 1993; revision received Jan. 25, 1994; accepted for publication Feb. 1, 1994.

*Associate Professor and Director, Department of Mechanical Engineering, 245, Sec. 3, Yenchiuyuan Rd.

†Assistant Research Scientist, Aero Industry Development Center, P.O. Box 90008-12-2.

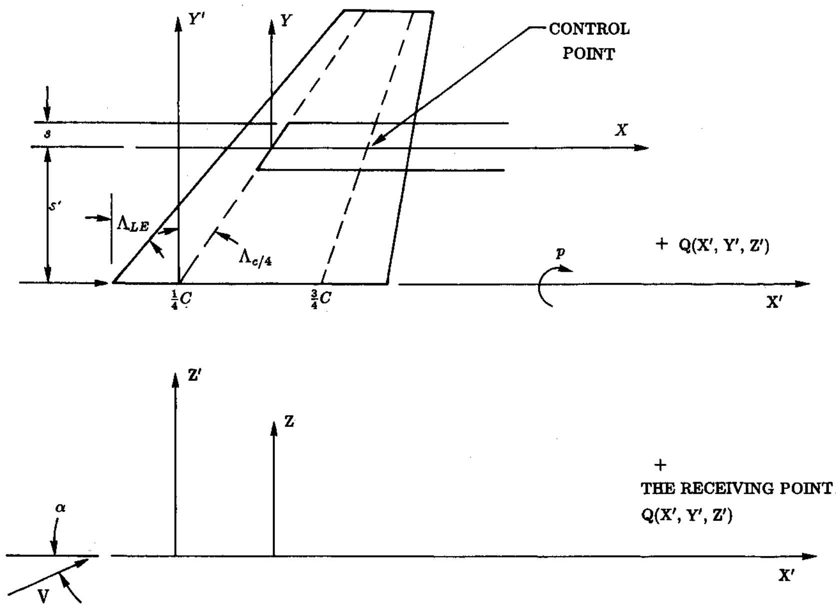

Fig. 1 Schematic diagram of vortex-lattice element on wing.

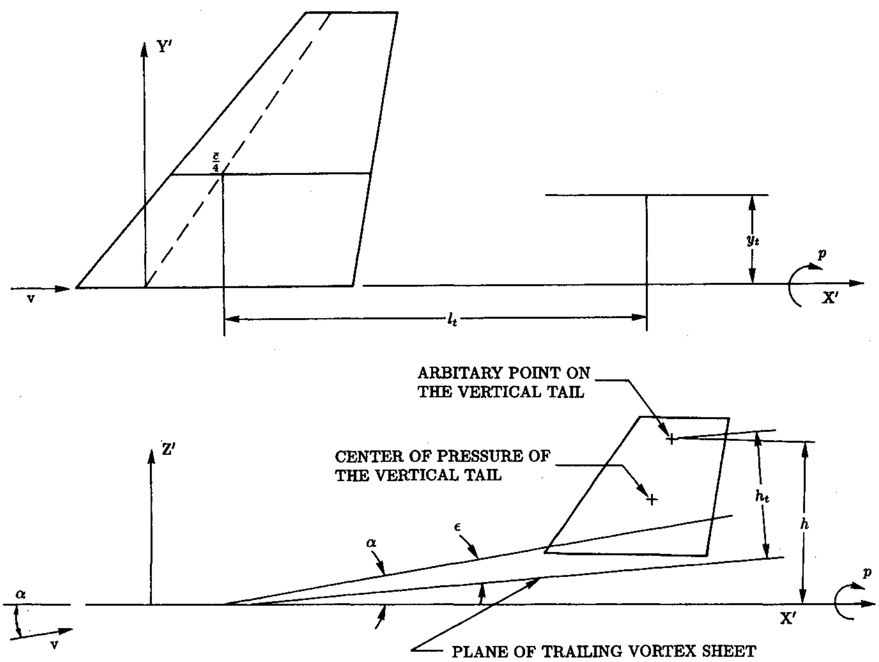

Fig. 2 Geometry definitions of wing and tails.

and aspect ratio, is limited to incompressible inviscid flows. Since most of the work on conventional vortex-lattice method concentrated on subsonic flows, the application of this basic technique of vortex-lattice theory to supersonic flows is extended and introduced to calculate the sidewash on the vertical tail of a fighter. Based on Miranda's technique,[9] the author combined the above generalized vortex-lattice method and will briefly discuss this later in this article. In addition, it is proved that the present method is suitable for the calculation of circulation distribution on the rolling wing and the sidewash on the vertical tail induced by the asymmetrical circulation distribution in subsonic and supersonic flows.

If the lifting surface and its wake are considered as being composed of a large number of discrete flat elements, and the element is replaced by the vortex filament γ_j, then the classical vortex-lattice method showed that the velocity field generated by the vortex filaments can be expressed as

$$V(\boldsymbol{R}) = -\frac{\beta^2}{2\pi K}\sum_{j=1}^{N}\gamma_j\delta_j\int_{c_j}\frac{\boldsymbol{R}-\boldsymbol{R}_1}{R_\beta^2}\,\mathrm{d}l \qquad (1)$$

The above equation is not appropriate for supersonic flows. We extended it by considering the contribution of the inherent singularity to the velocity field induced by the vortex element γ as w^*

$$w^* = (-\gamma\cos\Lambda/2)\sqrt{B^2 - t^2} \qquad (2)$$

This shows that w^* do have physical meaning when the vortex lines are swept in front of the Mach lines, i.e., $B^2 > t^2$. Combining Eqs. (2) and (1), and letting $K = 2$, the vortex-lattice method is now suitable for supersonic flows. For a noncamber wing without dihedral angle—after modeling—it can be replaced by a system of wing element with horseshoe vortices. The skewed horseshoe vortex is arranged as shown in Fig. 1, where the bounded vortex is placed on the quarterchord line and the trailing vortex lines are parallel to x axis. Although the trailing vortices will roll up when they leave the wing trailing edge in an actual case, the straight-line trailing vortices are assumed extending downstream to infinity for simplicity. For engineering applications, the aforementioned

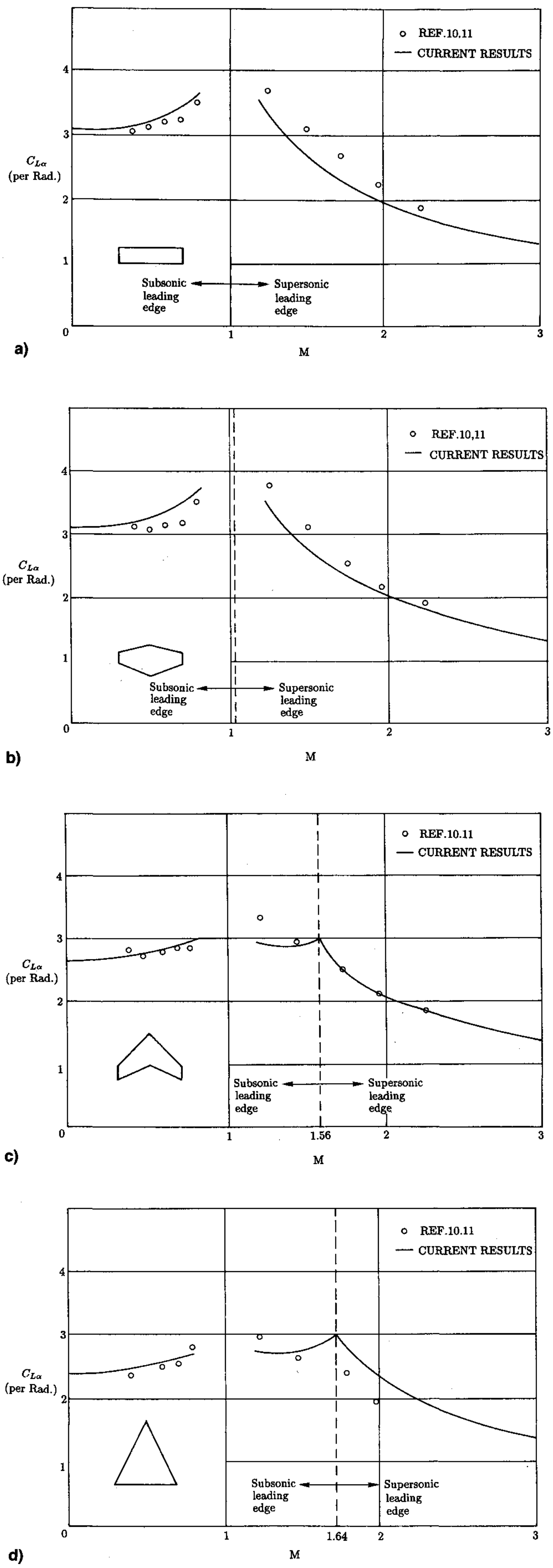

Fig. 3 **Comparison of lift curve slope: a) straight wing—*AR* = 2.75, $\Lambda_{c/4}$ = 0 deg, λ = 1.0; b) trapezoidal wing—*AR* = 2.75, $\Lambda_{c/4}$ = 0 deg, λ = 0.5; c) sweptback wing—*AR* = 2.75, $\Lambda_{c/4}$ = 50 deg, λ = 0.5; and d) delta wing—*AR* = 2.75, $\Lambda_{c/4}$ = 52.4 deg, λ = 0.**

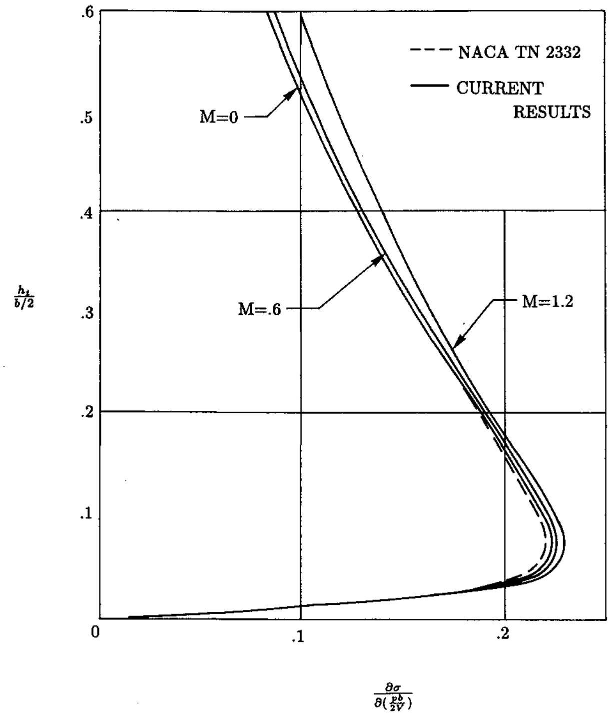

Fig. 4 **Current results and the comparisons with Michael's calculations; sweptback wing: *AR* = 3.5, $\Lambda_{c/4}$ = 60 deg, λ = 0.5, $l_t/b/2$ = 1.0.**

linear theory is always used and suitable accuracy can be obtained in the preliminary analysis.

The induced velocity at the receiving point $q(x_0, y_0, z_0)$ due to the skewed horseshoe vortex is given as

$$u = \frac{\Gamma Z_0 \beta^2}{2\pi K} \int_C \frac{dy}{\{(x - x_0)^2 + \beta^2[(y - y_0)^2 + z_0^2]\}^{3/2}} \tag{3a}$$

$$v = \frac{-\Gamma Z_0 \beta^2}{2\pi K} \int_C \frac{dx}{\{(x - x_0)^2 + \beta^2[(y - y_0)^2 + z_0^2]\}^{3/2}} \tag{3b}$$

$$w = \frac{\Gamma Z_0 \beta^2}{2\pi K} \int_C \frac{(x - x_0)\, dy - (y - y_0)\, dx}{\{(x - x_0)^2 + \beta^2[(y - y_0)^2 + z_0^2]\}^{3/2}} \tag{3c}$$

In order to integrate Eq. (3), the x coordinate appearing in Eq. (3) is assumed as $x = ty$ and the width of skewed horseshoe vortex is set as $2s$. The induced velocity contributed by the bounded vortex and the trailing vortices are then expressed as

$$u = \frac{\Gamma Z_0}{2\pi K} \frac{(F_1 - F_2)}{x^{*2} + (t^2 + \beta^2)z_0^2} \tag{4a}$$

$$v = \frac{\Gamma Z_0}{2\pi K} \left\{ -\frac{(F_1 - F_2)t}{x^{*2} + (t^2 + \beta^2)z_0^2} + \frac{G_1}{y_1^2 + z_0^2} - \frac{G_2}{y_2^2 + z_0^2} \right\} \tag{4b}$$

$$w = \frac{-\Gamma Z_0}{2\pi K} \left\{ \frac{x^*(F_1 - F_2)t}{x^{*2} + (t^2 + \beta^2)z_0^2} + \frac{y_1 G_1}{y_1^2 + z_0^2} - \frac{y_2 G_2}{y_2^2 + z_0^2} \right\} \tag{4c}$$

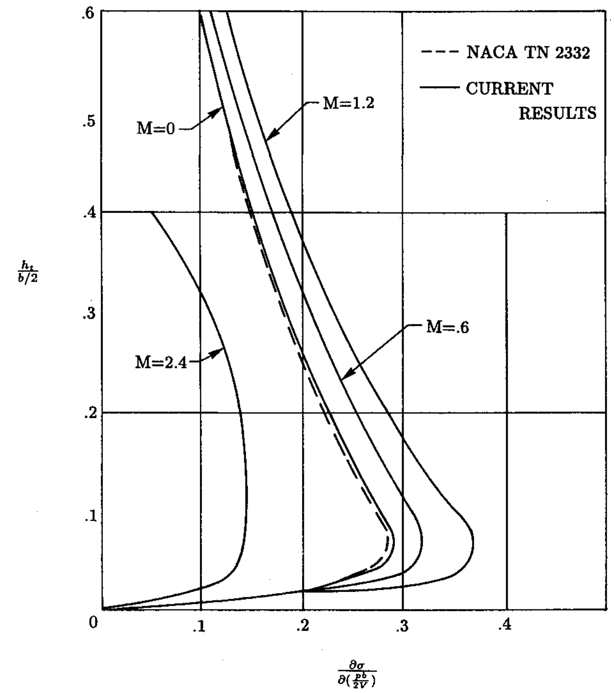

Fig. 5 Current results and the comparisons with Michael's calculations; straight wing: $AR = 6.0$, $\Lambda_{c/4} = 0$ deg, $\lambda = 1.0$, $l_t/b/2 = 1.0$.

where

$$x_1 = x_0 + ts, \quad x_2 = x_0 - ts, \quad x^* = x_0 - ty_0$$

$$y_1 = y_0 + s, \quad y_2 = y_0 - s$$

$$F_1 = \frac{tx_1 + \beta^2 y_1}{\sqrt{x_1^2 + \beta^2(y_1^2 + z_0^2)}} \qquad F_2 = \frac{tx_2 + \beta^2 y_2}{\sqrt{x_2^2 + \beta^2(y_2^2 + z_0^2)}}$$

$$G_1 = \frac{x_1}{\sqrt{x_1^2 + \beta^2(y_1^2 + z_0^2)}} + C(M_\infty < 1 \quad C = 1 \quad M_\infty > 1 \quad C = 0)$$

$$G_2 = \frac{x_2}{\sqrt{x_2^2 + \beta^2(y_2^2 + z_0^2)}} + C(M_\infty < 1 \quad C = 1 \quad M_\infty > 1 \quad C = 0)$$

Because the control point is placed on the midspan and the three-quarter-chord point of each wing element, the vertical component of the induced velocity on the control point is equal and opposite to the corresponding component of the incident flow. From Eq. (4c), the induced downwash at the control point due to the wings is

$$w_i = \sum_{j=1}^{N} D_{ij}T_j$$

or

$$[w]n \times 1 = [D]n \times n[\Gamma]n \times 1 \tag{5}$$

Using the boundary condition $w = -V\alpha$, Eq. (5) can be written as

$$[D]n \times n[\Gamma]n \times 1 = [-V\alpha]n \times 1 \tag{6}$$

If the wing is under a steady roll rate p, Eq. (6) becomes

$$[D]n \times n[\Gamma]n \times 1 = [-(V\alpha + ps')]n \times 1 \tag{7}$$

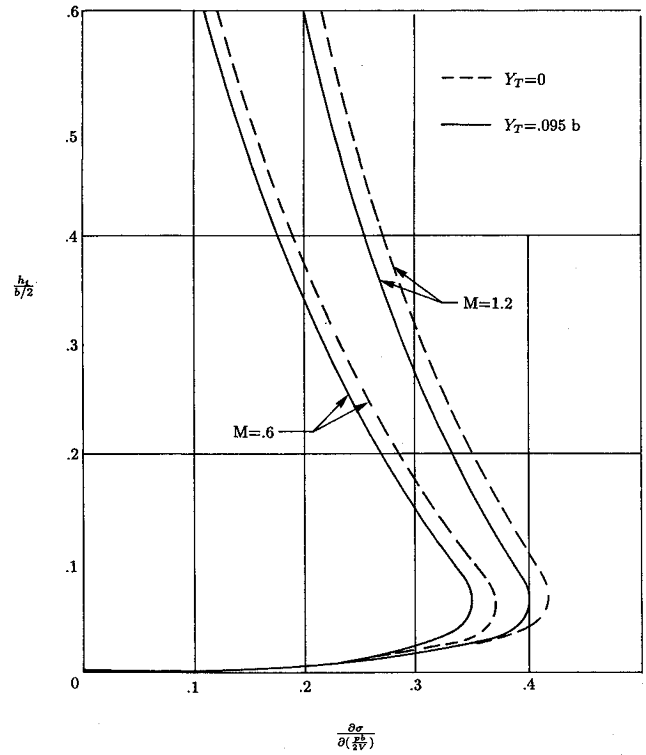

Fig. 6 Sidewash on the single and twin vertical tails in subsonic and supersonic flows; sweptback wing: $AR = 3.5$, $\Lambda_{c/4} = 27.7$ deg, $\lambda = 0.3$, $l_t/b/2 = 1.0$.

where s' is the distance between the symmetric axis of the wing element and the symmetric axis of the wing. In Eqs. (6) and (7), the unknown circulation can be solved after D is found from

$$[\Gamma]n \times 1 = [D]^{-1}n \times n[-V\alpha]n \times 1, \quad \text{nonrolling wing} \tag{8}$$

$$[\Gamma]n \times 1 = [D]^{-1}n \times n[-V\alpha + ps']n \times 1, \quad \text{rolling wing} \tag{9}$$

Sidewash on the Vertical Tail Due to Rolling Wing

In the calculation of the sidewash induced by the rolling wing, the effect of angle of attack must be taken into account. In addition, the circulation distribution on the wing, the displacement of the vertical tail, and the displacement of the trailing vortex sheet are directly influenced by the variation of angle of attack. It is seen that the additional symmetrical circulation distribution will not cause sidewash on the single vertical tail that is on the symmetrical plane. However, it actually causes sidewash on the twin vertical tails because of the asymmetrical locations of the tails.

If the wing is under a steady roll rate p, the circulation distribution on the wing can be obtained by Eq. (9). Because the circulation distribution is known, the induced sidewash velocity $v(x', y', z')$ on point $Q(x', y', z')$, due to the wing element, can be calculated by Eq. (4b). From Eq. (4b), the induced sidewash velocity $v(x', y', z')$ due to the wing is

$$v(x', y', z') = \sum_{j=1}^{N} S_j\Gamma_j \tag{10}$$

where j is the jth influencing wing element. The induced sidewash angle is

$$\sigma = \frac{v}{V} = \frac{1}{V}\sum_{j=1}^{N} S_j\Gamma_j \tag{11}$$

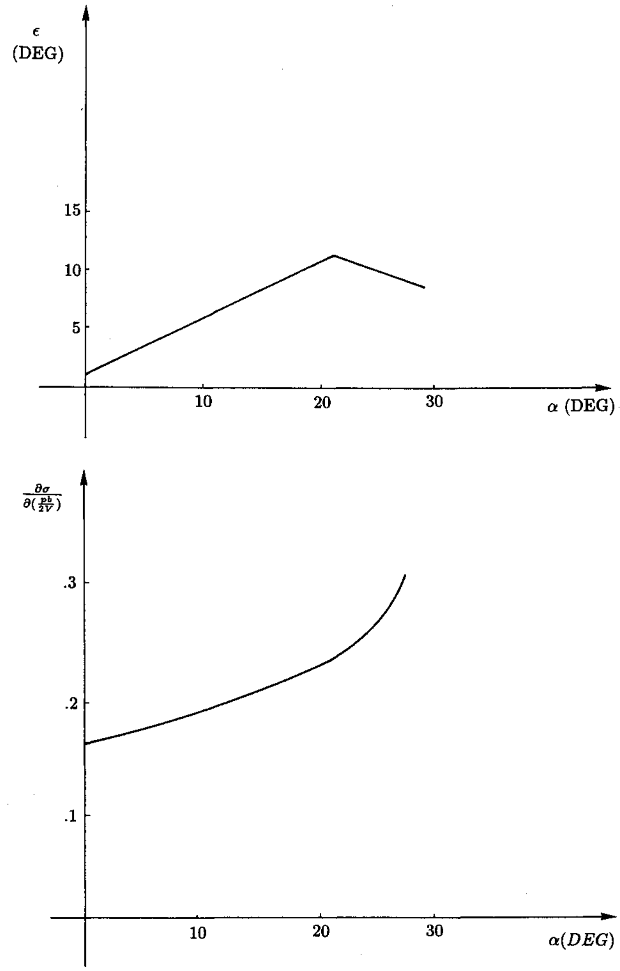

Fig. 7 Sidewash on the vertical tail due to rolling wing through high AOA; sweptback wing: AR = 4.82, Λ_{LE} = 11.25 deg, λ = 0.5, $l_t/b/2$ = 0.82, $h_t/b/2$ = 0.38 (an example).

and the nondimensional induced sidewash is

$$\frac{\partial\sigma}{\partial(pb/2V)} = \frac{2}{pb}\sum_{j=1}^{N} S_j\Gamma_j \tag{12}$$

In order to compare with Michael's calculations, the geometry definitions of wing and tails are defined as shown in Fig. 2.

Results and Discussion

The comparisons of current calculations and measurement results of lift curve slope are shown in Fig. 3.[10,11] A reasonably good result is obtained not only in subsonic flows, but also in supersonic flows. In Figs. 3a and 3b, the current results confirm the linear wing theory at subsonic and supersonic incident flow, and so the curves are monotonically smooth. But there is a gap on the $C_{L\alpha}$ curve for these two wings due to the linear theory limination of $M = 1$. In addition to this gap, there is a kink at $M = 1.56$ and 1.64 in Figs. 3c and 3d, respectively, for these two swept wings at supersonic incident flow, simply because the flow complexity at the normal Mach number equals around 1. Based on the present theory we only calculate the region outside the Mach cone. It can be seen that the swept effects do make significant contributions to the curve of $C_{L\alpha}$ vs M. The comparisons of some results between current calculations and Michael's result are shown in Figs. 4 and 5. A good agreement is obtained in incompressible inviscid flow. Figure 6 shows that the sidewash on the single vertical tail is greater than that on the twin vertical tails. From Figs. 4–6 it can be seen that the maximum sidewash occurs around $M = 1.0$. Figure 7 represents the sidewash on the vertical tail induced by a rolling airplane for α through 29 deg at $M = 0.2$. It seems that the current method will be helpful for spin and high angle-of-attack maneuver analysis of the fighter airplane.

Conclusions

The current calculations show that the sidewash on the vertical tails induced by the rolling wing is strongly affected by the wing geometry, the vertical tail location, the angle of attack, and the Mach number. For more accuracy, the downwash angle used in the calculation of sidewash should be measured from a wind-tunnel test. Combining the force model wind-tunnel test data and the sidewash calculated by the current method, the rolling dynamic derivatives can be evaluated effectively through high angle of attack and high Mach number.

References

[1]Lan, C. E., "Calculation of Lateral-Directional Stability Derivatives by a Nonplanar Quasi-Vortex-Lattice Method," NASA CR-165659, 1981.

[2]Lan, C. E., "The Unsteady Suction Analogy and Applications," AIAA Paper 81-1875R, 1981.

[3]Ellision, E. E., "USAF Stability and Control Handbook (DATCOM)," Air Force Flight Dynamics Lab., AFFDL/FDCC, Wright-Patterson AFB, OH, June 1969.

[4]Roskam, J., "Airplane Flight Dynamics and Automatic Flight Controls," Roskam Aviation and Engineering Corp, Pt. 1, Lawrence, KA, 1979, pp. 193–199.

[5]Wykes, J. H., Casteel, G. R., and Collins, R. A., "An Analytic Study of the Dynamics of Spinning Aircraft," Pt. I, WADC TR 58-381(I), 1958.

[6]Michael, W. H., Jr., "Analysis of the Effects of Wing Interference on Tail Contribution to the Rolling Derivatives," NASA TN-2332, 1951.

[7]Liu, H. I., and Chiu, C. S., "An Investigation of Sidewash on the Vertical Tail Due to Rolling Wing," 9th National Conf. on Theoretical and Applied Mechanics, STAMROC-9-305, Taipei, Taiwan, Republic of China, Dec. 1958.

[8]Weissinger, J., "The Lift Distribution of Sweptback Wings," NACA TM-1120.

[9]Miranda, L. R., Elliot, R. D., and Baker, W. M., "A Generalized Vortex Lattice Method for Subsonic and Supersonic Flow Applications," NASA CR 2865, 1977.

[10]Becker, E., and Wedemeyer, E., "Untersuchungen an funt Flugeln mit verchiedener Umrissform bei hohen unterschallgesch windigkeiten," Jb. WGL, 128, 129; Z. Flugw., 8:44–52, 1960; Kowalke, F.: Jb. WGL, 40–48, 1958; Krause, F.: Flugw., 12:263–273, 1964.

[11]Stahl, W., and Mackrodt, P. A., "Dreikomponenten-Messungen bis zu grossen anstellwinkein an funt Tragflugeln mit verschieenen Umrissformen in Unterschall-und Uberschall-Stromung," Z. Flugw., 11:150–160, 1963; 13:447–453, 1965; Jb. WGLR, 159, 1962; Lipowski, K.: Z. Flugw., 13:453–458, 1965.